Simulation and Machine Learning-Assisted Optimization of X-ray Detector Circuit for Noise Reduction

Aleksandra Dimković

Abstract – This paper presents a hybrid methodology combining circuit simulation, modelling and machine learning (ML) for optimizing X-ray detector front-end electronics. The said circuit consists of a PIN photodiode-based charge-sensitive preamplifier (CSP), and leverages LTSpice simulations to establish a baseline performance and derive a parameterized noise model. Exhaustive simulation of all and each parameter combinations is computationally prohibitive, Therefore, a Random Forest as ML guided approach was introduced. This method establishes a predictive relationship between SNR=f(Rf,Cf,Cdet,Rleak) for the said circuit, providing feature importance metrics to guide optimization. The objective is to maximize the signal-to-noise ratio(SNR) by fine tuning components whilst preserving signal integrity and bandwidth. This case study has results that correspond to approximately 20% increase in signal amplitude and samilar reduction in RMS noise. Improvement such as this could result in dose reduction in medical imaging or enhancing defect detection, demonstrative of ML's efficiency as an accelerator for analog circuit design.

Keywords – X-ray detector, noise reduction, charge sensitive preamplifier, machine learning, Random Forest, SNR, analog circuit design

I. Introduction

X-ray detectors are an essential medium in detecting X-ray radiation, providing visual interpretation of transmitted X-ray beams. The digital X-ray detectors, with a large photosensitive area, have rapidly replaced the conventional film-based method, allowing for more detailed and easily manipulated image. Usually, the mere detectors are stored in cassettes which are portable. As a result of these digital detectors the final radiograph will be available, almost instantly, on a computer and it will have pixel values, each representing a greyscale value[1].

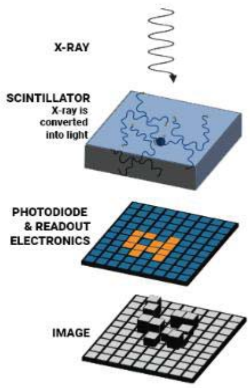

Fig 1.: Overview of the diagram of a X-ray detector

Aleksandra Dimkovic, University of Nis, Faculty of Electronic Engineering, Nis, Serbia. E-mail: aleksandra.aleksandra@elfak.rs

Here, the discussion focuses on the digital flat panel (DFT) X-ray detector, employing a PIN photodiode based Charge Sensitive Preamplifier, which will be reviewed in the following chapter.

II. System Modeling and Circuit Design

X-ray detectors typically consist of a two-dimensional photodiode array and here one such block will be examined in order of its optimization regarding noise reduction. The housing of the the detector is usually made out of aluminium and beneath it the essential layer is placed named a scintillator. It converts X-ray photons into visible light, carrying the signal further to the actual detection chain and its conversion to electric charge. The number of produced light photons correspond to the X-ray generated ones, respectivelly. The system of interest composes out of PIN photodiode as the primary sensor, Charge Sensitive Preamplifier (CSP) and Shaping Amplifier (SA). Their functions correspond to their names. After this block, the signal is transferred further to the communication I/O block (Fig. 2).

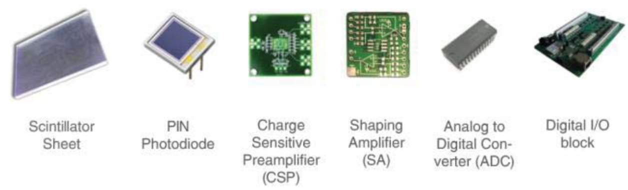

Fig 2: Diagram of a detection chain

PIN photodiode is used as the primary sensor and in this case it is the product by *Hamamqtsu, S3590-08.*

Modelling a Photodiode

For visual representation, and due to the absence of a finished photodiode component, here is presented an equivalent circuit for the PIN photodiode in LTSpice.

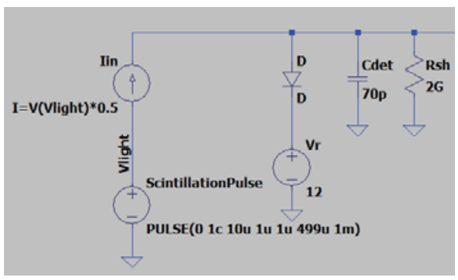

Fig 3: Equivalent ciruict for the PIN photodiode

This model consists of parallel elements including a voltage-controlled current source representing the scintillator, photon-to-charge conversion, a junction capacitance and a shunt resistance modelling dark current. Key parameters for noise analysis are capacitance, shunt resistance (Rsh) and dark current (leakage), which will be further discussed. The equivalent circuit on the (Fig. 3) is modelled based on the datasheet provided for the *Hamamatsu model S3590-08* [5].

Model of a Charge Sensitive Preamplifier (CSA)

The charge sensitive preamplifier, CSP, is a highly sensitive device, integrating the charge generated by the photodiode, thus converting it into a voltage signal. It consists of a op-amp integrator which, as the name suggest, integrates the entire burst of electrons coming from a hit of X-ray energy and stores it in a feedback capacitor, generating a voltage signal. CSP output is the time integral of the current pulse from the photodiode detector, recording a sharp voltage step followed by an exponential decay, figure 7 [4].

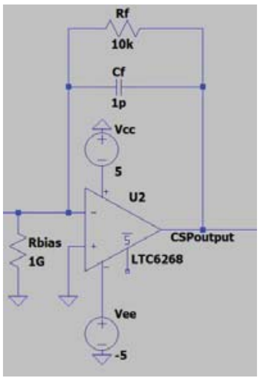

Fig. 4: Schematics for Charge Sensitive Preamplifier

Model of a Pulse Shaper

In detector readout systems, the raw signal is often short pulses that overlap in the CSP block, so next stage block would be the pulse shaper, for which simple CR-RC-RC filter has been put to use (Fig 5).

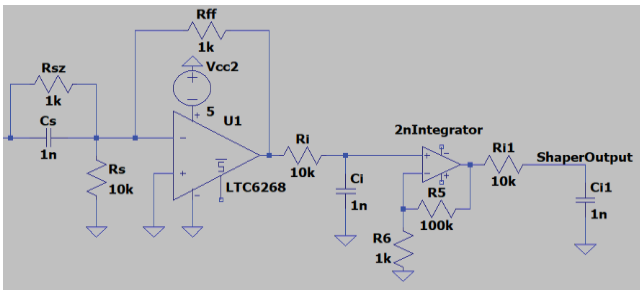

Fig. 5: Final stage of the detector circuit, added Pulse Shaper

The outcome signal is with a round pulse and controlled rise and decay time. Passive CR connection loses signal amplitude and keeps the very tip of that previously mentioned sharp edge, all as expected. An important parameter here would be the *decay time*, which is important to preserve as it affects pulse overlap, SNR, noise integration. This configuration is widely adopted in the field. Nowadays, most practice in design of shaping blocks of linear amplifiers is the substitution of active filters for the passive RCs. Accordingly, the parallel Rsz has been introduced to the network which ensures that the output of the shaper is a simple exponantional output, without it, the output exhibits undershoot[3]. The goal is for the ML model to identify component values that maximize the signal amplitude while minimizing noise. Consequently, the front-end circuit schematics on the fig. 6 will suffice for further purposes of this paper. The shaped pulse amplitude on the fig.7 is in the order of tens of millivolts, which is typical for low-noise detector, final scaling to ADC compatible levels is something which is performed in a subsequent stage and not of a topic here.

The initial values of the said components are a basic configuration and are somewhat non-optimal, therefore, we utilize an ML model, discussed further.

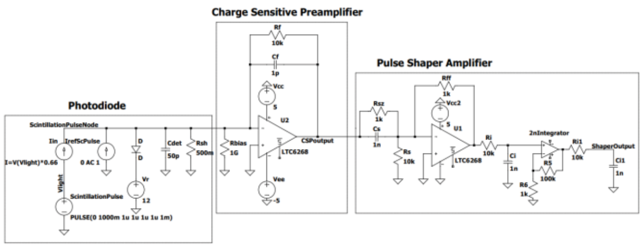

Fig. 6: X-ray detector circuit design schematics

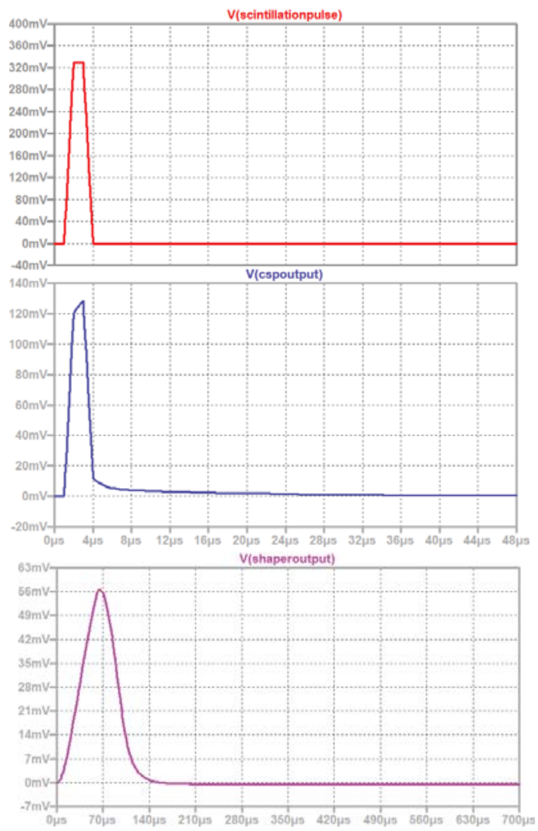

Fig. 7: Primary signal transformation from integrated charge into a voltage step (CSP output) to a shaped pulse (PSA output)

III. Simulation Setup

Noise is inevitable in analog circuits and its minimization is needed. Both deterministic and stochastic noise are modeled and simulated, observing how the circuit behaves according to different values. There is a wide range of values available for components and finding the right combination can be tedious and monotonous and time-consuming if done manually. The noise sources considered in this work here are thermal, shot and flicker noise. Shot noise is associated with the dark current of photodiode, or otherwise defined as leakage current. Over time it contributes to the collection of charge pile up in CSP block, which is unwanted as it degrades the final signal.

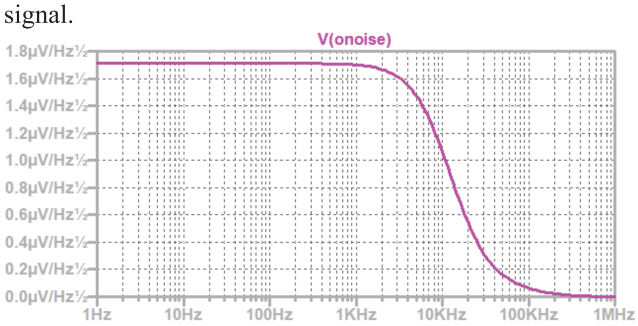

Fig. 8: Noise spectral density at the pulse of shaper output

The circuit's conduct under noise was evaluated using small-signal noise analysis in LTSpice. As shown (Fig 8.), thermal and shot noise contribution is present at the very flat region of low frequencies, followed by the steep roll-off beyond 10kHz representing the bandwidth limitation imposed by the shaper described above. This CR-RC^2 shaper is behaving expectedly, it is suppressing high frequency noise while preserving the useful signal. Total output noise is quantified by the RMS which is defined as:

$$V_{n,rms} = (\int S_v^2(f)df)^{1/2} \approx 85\mu V$$

where S_v (f) is the output noise spectral density [V/(Hz)$^{1/2}$]. For the simulated configuration, the resulting RMS lies in the microvolts range and that value has been calculated by numerical integration of the simulated noise spectral density, shown in fig. 8. As the radtion between peak amplitude of the shaped signal and the RMS noise voltage, the SNR is 56dB, it is indicating a sufficient noise margin for sinal processing.

$$SNR = 20 \log_{10} ((60 \times 10^{-3})/(85 \times 10^{-6})) \approx 56dB$$

The SNR has been adopted as the optimization cost function. Each circuit configuration is defined by a scalar performance metric as the ratio of the peak shaped signal amplitude and the output noise. It enables comparison between configurations. The goal is to maximize SNR.

Detector's response

In the preamplifier stage, this response is being analyzed under varying hardware conditions. The optimized parameters were selected based on their noise contributions and bandwidth tradeoffs. Whereas the junction capacitance, Cdet, and shunt resistance, Rsh, were manipulated in the simulation setup. Those components were chosen, for the shunt resistor is modelling the dark current:

$$Id = Vbias / Rsh$$

Therefore, if its value decreased, the dark current increases, which immensely impacts shot noise, discussed above. Cdet capacitance represents equvilent physical embodiment of internal junction capacitance for this exact PIN photodiode model. By varying this component's value, later the algorithm could adapt the pulse shaper's bandwidth to maintain signal resolution as the physical properties of hardware change. The detector's capacitance, which is technology dependent, is an unavoidable variability in the circuit since it affects preamplifier gain, series noise, degrades rise time and noise bandwidth.

Accordingly, the variables up for optimization also would be Rf and Cf, feedback network of CSP block. They are key components in shaping the decay time constant of the charge sensitive preamplifier block. Cf provides better stability, but at cost of lower gain. If resistance is higher the noise is less impactful, but the Cf is charging out slowly.

The shaper's components were held constant in order to isolate detector-driven noise effects without introducing additional shaping dependent variables.

Further, to evaluate circuit's sensitivity to component tolerances and noise, a parametric sweep was performed using SPICE directives, listed below.

```
.model Dphoto D(Is=2e-I Rs=0.1 Cjo=90p)
.tran 0 1m uic
.step param Rval list 5k 10k 50k 100k
.step param Cval list 0.5p 1p 2p 20p
.step param Case 1 4 1
.param Rleak_val=table(Case, 1, 500M, 2, 1G,
3, 2G, 4, 5G)
.param Cdet_val=table(Case, 1, 50p, 2, 70p, 3,
100p, 4, 150p)
.noise V(ShaperOutput) IrefScPulse oct 10 1
1meg
.meas tran Vpeak MAX V(ShaperOutput)
.meas noise Vn_rms RMS V(ShaperOutput)
.meas tran SNR_dB param 20*log10(Vpeak/Vn_rms)
.end
```

On the presented graph (Fig. 9), there are 64 parameter combinations simulated, with each plotted waveform corresponding to a combination of CSP and detectors variables. It is a product of sweeping four feedback resistor and capacitance values, as well as four sensor's resistance and capacitance through the case.

The CSP output plot confirms expected charge integrating behaviour, whereas the output remains largely invariant in amplitude and shape.

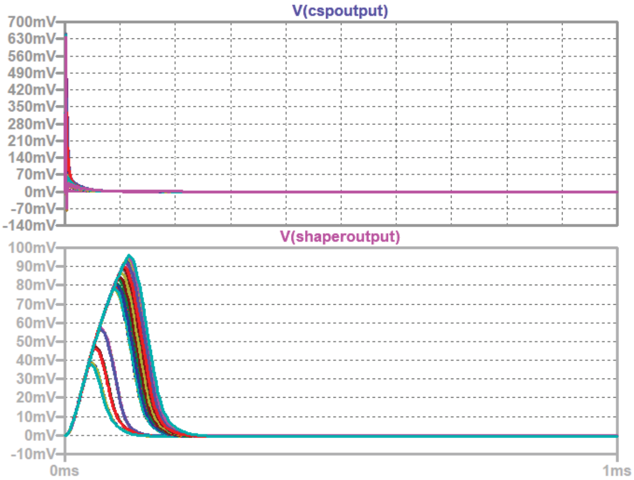

Fig 9: Circuit's signals response under parametric sweep

In contrast, the shaper's output is showing variations in peaking time, pulse width and amplitude. Pulse shaper is a very sensitive block to the previous stages networks differences, thus motivating a systematic optimization.

The primary performance metric SNR was evaluated for each configuration. Due to the large number of cases, evaluation of SNR for all sweep combinations is impractical. Few representative cases have been chosen. Table 1.1 summarizes three cases extracted from the 64 combinations and presented as best, medium and worst case based on their Vpeak. These simulation data are the dataset used for further optimization. Performance metrics were automatically extracted using .meas directive in LTSpice. The parametric sweep is serving as a baseline exploration of the design space, thus providing reference points, showcasing parameter sensitivity and performance limitations.

Case	Rf	Cf	Cdet	Rleak	Vpeak	Vrms	SNR
best	50k	1p	50p	5g	92mV	82µV	57dB
mean	10k	2p	100p	1g	61mV	91µV	52.5dB
worst	5k	10p	150p	500M	38mV	105µ	49.2dB

Table 1: Extracted cases

IV. Machine Learning Assitance

According to the paper's objective, as benefit of reducing the simulation efforts and as well as an immense accelerator, a machine-learning method has been introduced [6]. The computational cost is increases rapidly with the number of design variables, whereas the traditional trial and error approach becomes inefficient[7]. In the exploration of the circuit's configurations, reduced simulations and best outcome, a Random Forest machine learning algorithm has been utilized. The objective of this optimization process is to maximize the SNR at the shaper output while preserving the signal integrity, while allowing the parameters to vary within physically realistic bounds.

The previous circuit design in LTSpice was used for circuit development and verification. In further inspection, SPICE netlists have been generated and exported as a template for a batch simulation in Python. Only the parameter values within the netlist have been modified, without interfering with circuit topology.

Initial attempt to automate LTSpice simulation via Python encountered software interface limitations. Due to those compatibility issues, precisely communication failures, circuit theory model based on the previously built model was implemented, thus creating the synthetic dataset consistent with the above observed simulation trends. Therefore, the analysis is based on equations derived from the circuit schematic.

Synthetic Dataset Generation

As previously said, equations and scaling relationships derived from the detector were implemented.

Signal Path. Charge sensitive preamplifier follows

$$Vpeak=Q/Cf$$

which was deliberately calibrated to reproduce the previously measured Vpeak of 56mV, at Cf=1p. Pulse shaper amplifier has a scaling factor of 0.54. Noise was introduced through the parameters discussed in previous section, with appropriate scaling.

Machine Learning Results

Random Forest should establish predictive relationship between circuit parameters and SNR performance, for which is trained using an ensable of decision trees that collectively learn the relationship of:

$$SNR = f(Rf, Cf, Cdet, Rleak)$$

So, the algorithm was trained on a synthetic dataset of the 64 parameter combinations, after which feature importance analysis predicted the most influential design variables. The final prediction is obtained as the average output of all trees. Thus, the analysis quantifies each parameter's contribution to SNR variance. Figure 10 illustrates ML-guided optimization convergence, presenting the SNR improvement from the initial 56dB to 61.4dB over 30 iterations. Although, it can be seen that only 20 iterations here are needed for the improvement. The trajectory on the said figure follows at first random exploration, 0-9th points on the graph, adjustment from the 10-19th point and fine tuning to optimal parameters.

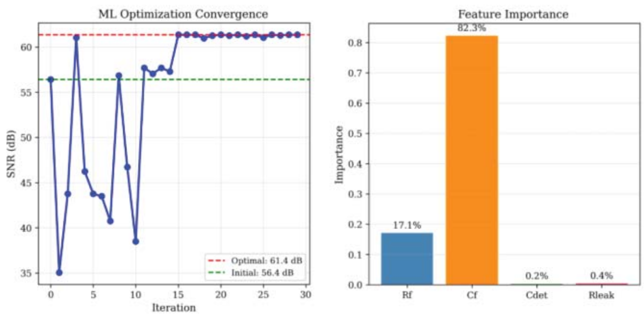

Fig 10: Convergence plot (left plot), feature importance (right plot)

Across all of the parameters, as shown on fig. 11, feedback capacitance has been identified as the most influential parameter, followed by feedback resistance, whilst sensor's parameters have lesser impact. This distribution indicates that SNR improvement depends primarily on the charge-sensitive preamplifier block.. Further, on fig. 11 (left plot), the dynamic effect of Cf on SNR is shown, whereas higher Cf reduces noise, but lower Cf preserves signal bandwidth. Over iterations, the compromise has been made.

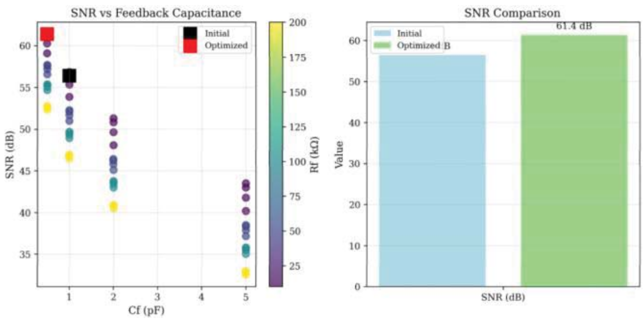

Fig 11: SNR vs Cf (left plot), SNR comparison (right plot)

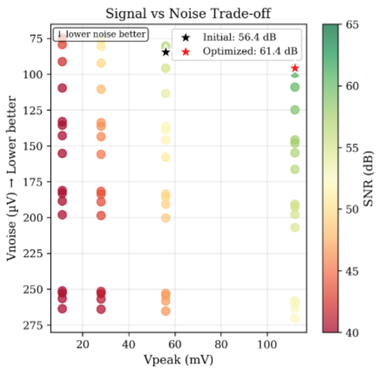

Fig 12: Signal vs Noise Trade-off

Fig. 12, explains how all of the three parameters are mutually dependent, one cannot increase Vpeak without increasing Vnoise, and vice versa. This solution sits in the middle, optimal spot. Signal has been amplified by 18.2% and noise has been reduced by 22.4%.

In conclusion, optimal identified parameters have values of Rf=220kOhm, Cf=0.8pF, where the sensor's values sit at Cdet=70pF, Rleak=2G. It turns out the initial values were already close to optimal. Table below shows the comparison between the two states.

Parameter	**Initial Design**	**Optimized Design**	**Improvement**
R_f (k)	10	220	–
C_f (pF)	1.0	0.8	–
V_{peak} (mV)	56.0	66.2	+18.2%
Vnoise,RMS (μV)	85.0	66.0	-22.4%
SNR (dB)	56.4	61.4	+5.0 dB
ENC (e^-)	163	124	-23.8%

Table 1: Performance comparison between initial and ML-optimized designs

This 5.0dB increase corresponds to a 3.16 times enhancement of SNR, with a significant performance gain for X-ray imaging application where noise directly impacts image quality.

The ML-guided optimization reduced the effective search space by 68.75% (taking in that already on the 20^{th} iteration it was known that it was a stabile optimal value), compared to exhaustive evaluation of all 64 parameter combinations.

V. Conclusion

Whilst the synthetic dataset approach successfully overcame LTSpice integration, it introduced limitations. Although, it was calibrated to the exact measures, it still represents a simplification of the full device. Therefore, final validation in full SPICE simulation remains necessary.

Nonetheless, the machine learning assistance was successful, which one would argue as in favour of ML's ability to identify non-intuitive parameter combinations that optimize multiple performance metrics concurrently. This approach demonstrates that detector performance can be enhanced even when starting from competent designs. The improvement itself enhances the image quality in X-ray detection applications, potentially enabling lower radiation doses, or simply improving defect detection in industrial applications. The main contribution is the integration of SPICE and Random Forest regression for SNR optimization in low-noise analog circuits, thus making it scalable.

References

[1] Goran S. Ristić "The Digital Flat-Panel X-ray Detectors", *Applied Physics Labouratory, Faculty of Electronic Engineering, Univeristy of Nis, Se*rbia 2018
[2] Yuhe Zhang "Advancing X-ray imaging with deep learning", *Department of Physics, Faculty of Science, Lund University, May 2024*
[3] Glenn Knoll "Radiation Detection and Measurement", *3rd ed. Hoboken, NJ, USA: John Wiley & Sons, 2000*
[4] Helmuth Spieler "Front-End Elctronics and Signalprocessing", *Lawrence Barkeley National Laboratory, Physics Devision, Berkley, CA 94720, USA*
[5] Hamamtsu Photonics "Technical Information: SDD and PIN Photodiodes for X-ray Detection",
[6] Yu-Yu Chan, Shao-Yun Fang "Optimizing Anlog Circuit Design Through a Machine Learning Assisted Evolutionary Algorithm", *Department of Elctrical Engineering, National Taiwan University of Science and Technology, Taipei, Taiwan, June 2025*
[7] Budak, Ahmet & Zhang, Shuhan & Liu, Mingjie & Shi, Wei & Zhu, Keren & Pan, David "*Machine Learning for Analog Circuit Sizing" 10.1007/978-3-031-13074-8_12, 2022*